Published in final edited form as:
Dev Biol. 2005 August 15; 284(2): 464–478. doi:10.1016/j.ydbio.2005.06.010.

Multiple requirements for *Hes1* during early eye formation

Hae Young Lee[a,1,2], **Emily Wroblewski**[a,1,3], **Gary T. Philips**[b,4], **Carrie N. Stair**[b], **Kevin Conley**[c,d], **Meredith Reedy**[c,d], **Grant S. Mastick**[b], and **Nadean L. Brown**[a,c,d,*]

[a]Department of Pediatrics, Northwestern University Medical School at Children's Memorial Institute for Education and Research, Chicago, IL 60614, USA

[b]Department of Biology, University of Nevada, Reno, NV 89557, USA

[c]Divisions of Developmental Biology and Ophthalmology, Children's Hospital Research Foundation, Cincinnati, OH 45229, USA

[d]Department of Pediatrics, University of Cincinnati Medical School, Cincinnati, OH 45229, USA

Abstract

During embryogenesis, multiple developmental processes are integrated through their precise temporal regulation. *Hes1* is a transcriptional repressor that regulates the timing of mammalian retinal neurogenesis. However, roles for *Hes1* in early eye development have not been well defined. Here, we show that *Hes1* is expressed in the forming lens, optic vesicle, cup, and pigmented epithelium and is necessary for proper growth, morphogenesis, and differentiation of these tissues. Because *Hes1* is required throughout the eye, we investigated its interaction with *Pax6*. *Hes1–Pax6* double mutant embryos are eyeless suggesting these genes are coordinately required for initial morphogenesis and outgrowth of the optic vesicle. In *Hes1* mutants, *Math5* expression is precocious along with retinal ganglion cell, amacrine, and horizontal neuron formation. In contrast to apparent cooperativity between *Pax6* and *Hes1* during morphogenesis, each gene regulates *Math5* and RGC genesis independently. Together, these studies demonstrate that *Hes1*, like *Pax6*, simultaneously regulates multiple developmental processes during optic development.

Keywords

Optic vesicle; Lens; Morphogenesis; Neurogenesis; bHLH; Mouse; Hes1; Pax6; Math5

Introduction

Mouse eye development begins with complex morphogenetic events within the anterior neural plate at embryonic day 8.5 (E8.5). These include neural plate fusion, optic pit

*Corresponding author. Division of Developmental Biology, Children's Hospital Research Foundation, 3333 Burnet Avenue, Cincinnati, OH 45229, USA. Fax: +1 513 636 4317. nadean.brown@cchmc.org (N.L. Brown).
[1]These authors contributed equally to this work.
[2]Present address: Developmental Genetics Ph.D. Program, Columbia University, New York, NY, USA.
[3]Present address: Ecology, Evolution, and Behavior Ph.D. Program, University of Minnesota, St. Paul, MN, USA.
[4]Present address: Neurobiology and Behavior Ph.D. Program, University of California at Irvine, Irvine, CA, USA.

evagination, vesicle evagination to contact the surface ectoderm, optic vesicle constriction to create the optic stalk, optic vesicle growth, and lens invagination. Spatial organization and tissue specification are apparent by E9.5 (Chen and Cepko, 2000; Furukawa et al., 1997; Mathers et al., 1997; Nornes et al., 1990; Steingrimsson et al., 1994; Tachibana et al., 1994). At E10.5, a bilayered cup, composed of retinal pigmented epithelium (RPE) and presumptive neural retina, is connected to the brain via the optic stalk. Retinal neurogenesis initiates at early E11 in the dorso-central optic cup, with the appearance of the proneural gene *Math5* (Brown et al., 1998), followed by terminal division, differentiation, and migration of the first retinal neurons, retinal ganglion cells (RGCs) at late E12.5 (Hinds and Hinds, 1974; Rapaport et al., 2004). Therefore, early eye formation involves precise temporal orchestration of growth, specification, morphogenesis, patterning, and neurogenesis.

Retinal progenitor cells are initially multipotent for neuronal and glial fates, but subsequently pass through competence states that restrict available fates across time (reviewed in Livesey and Cepko, 2001). This model arose from multiple demonstrations that progenitors use inherent gene expression, positional information, and cell–cell interactions to adopt particular neuron identities (Holt et al., 1988; Turner and Cepko, 1987; Turner et al., 1990; Wetts and Fraser, 1988). The retinal environment changes over time, partly due to the appearance of differentiated neurons that express extrinsic factors. However, intrinsic proteins help determine progenitor competence states and both homeobox and basic helix–loop–helix (bHLH) transcription factors function in this process (reviewed in Akagi et al., 2004; Vetter and Brown, 2001). In the developing mouse retina, five neuron-promoting bHLH genes have been identified: *Math5*, *Ngn2*, *Math3*, *NeuroD*, and *Mash1*. The expression of each proneural gene coincides with a peak of genesis for a distinct retinal cell type(s). The activation of these genes occurs in a particular order, separated from each other by one day of development (Brown et al., 1998). Mammalian retinal progenitors that express one or more bHLH genes become biased to particular cell fates (Brown et al., 2001; Hatakeyama et al., 2001; Inoue et al., 2002; Marquardt et al., 2001; Morrow et al., 1999; Tomita et al., 1996b; Wang et al., 2001). For example, both loss- and gain-of-function studies demonstrate that *Math5* (*Atoh7*) promotes RGC fate (Brown et al., 2001; Liu et al., 2001; Wang et al., 2001).

The temporal control of retinal neurogenesis is not well understood. One temporal regulator, *Hes1*, is a transcriptional repressor of neurogenesis (reviewed in Kageyama et al., 2000) but also promotes Müller glia formation (Furukawa et al., 2000). *Hes1* is a mammalian homolog of *Drosophila hairy* and *Enhancer of split* that inhibit fly neurogenesis (Ishibashi et al., 1994, 1995). The *Hes*, *hairy*, and *Enhancer of split* genes all encode bHLH-O proteins with basic helix–loop–helix (bHLH), orange and WRPW domains (reviewed in Davis and Turner, 2001). Loss- and gain-of-function studies in the late embryonic and postnatal mouse retina demonstrate that *Hes1* represses the formation of RGC, rod, horizontal, and amacrine neurons (Hatakeyama et al., 2004; Tomita et al., 1996a). However, *Hes1* function during the earliest stages of eye development remains incompletely defined. Optic cup and lens defects, plus precocious neurons, were found in E10.5 *Hes1*−/− eyes (Tomita et al., 1996a), but these phenotypes have not been further investigated. Obvious morphological deformities at this

stage suggest a very early requirement for *Hes1* function. Recently, *Hes1* was identified as a clock molecule in vitro and in vivo, regulating its own expression through oscillation of mRNA and protein (Hirata et al., 2002). Although *Hes1* and other members of the *Notch* signaling pathway exhibit periodic expression during somite formation, the downstream effectors of oscillatory gene pathways are largely unknown. Together, these unanswered questions provoked us to examine further the roles of *Hes1* during early eye formation.

Here, we demonstrate that *Hes1* coordinates the timing of multiple processes at the earliest stages of mammalian eye development. In *Hes1* mutant mice, eye development is abnormal at E9.5, with alterations in lens, optic vesicle, and RPE formation. Ectopic retinal neurons were also observed in heterozygous and homozygous *Hes1* mutants at E9.5. Many neurons adopt an RGC fate, consistent with accelerated *Math5* expression. This was followed by the appearance of precocious amacrine and horizontal cells, recapitulating the wild type sequence. The multiple functions for *Hes1* are reminiscent of those of *Pax6* (Hill et al., 1991), and thus we explored the genetic relationship between these genes. While *Pax6* and *Hes1* oppositely regulate *Math5* and RGC genesis, they act coordinately during optic vesicle and lens morphogenesis. Together our findings demonstrate multiple and diverse functions for *Hes1* in the early embryonic eye.

Materials and methods

Animals

The *Hes1* targeted deletion (Ishibashi et al., 1996) is embryonic lethal, with variable phenotypes that are attributed to a nonstandard background (129J × CD1) and maintenance on an ICR background. Eye morphology and size were variable but accelerated neural development was seen in all mutant embryos. Embryos were obtained by mating *Hes1*+/− mice (E0.5 = day of vaginal plug), with dissection, fixation, and processing as in Brown et al. (1998). Embryo or adult genotypes were determined by PCR (Brown et al., 1998, 2001; Cau et al., 2000), using tail or extraembryonic tissue DNA. Somite-matched wild type, heterozygous, and mutant embryos were used in all experiments.

Compound mouse strains

To examine *Math5-LacZk.i.* expression in *Hes1* mutant embryos, *Math5*+/− mice in a CD-1 background (>N7 generations) were mated to *Hes1*+/− mice in an ICR background. All embryos came from the intercross of *Math5*+/−;*Hes1*+/− N1 mice. *Hes1-Pax6* mutants were created by mating Sey^{Neu}/+ mice (Hill et al., 1991), in an FVB/N background (>N7 generations), to *Hes1*+/− mice described above. All embryos were from the intercross of *Hes1*+/−;Sey^{Neu}/+ N1 animals. Genotypes were determined by PCR, using tail or extraembryonic DNA.

In situ hybridization and LacZ detection

Whole-mount in situ labeling used *Math5, Mash1, Ngn2, NeuroD, Pax6, Hes1, Mitf, Dct, Tyrp1*, and *Rx* cRNA probes (Brown et al., 1998; Hargrave and Koopman, 2000). To detect Math5-k.i. LacZ expression, x-gal staining (Sanes et al., 1986) was performed. Embryos were imaged using Spot RT or Magnafire digital image cameras and Adobe Photoshop 7.0

software. Embryos were embedded in gelatin/sucrose/PBS, cryosectioned at 10 μm and imaged with a Leica microscope, Orca camera, Openlab 3, and Adobe Photoshop 7.0 software.

Immunohistochemistry

Fixed embryos were washed through a sucrose gradient, embedded in 15% sucrose/7.5% gelatin/0.1 M phosphate or OCT, and cryosectioned at 10 μm. Sections of retinal tissue were processed for antibody labeling as in Mastick and Andrews (2001). A rabbit polyclonal antibody was raised against a C-terminal peptide of the mouse Hes1 protein (amino acids 264–283) and purified by affinity chromatography (Invitrogen). This antisera was used at 1:1000 on embryo sections that were fixed 1 h with 4% PFA/PBS. Other primary antibodies used were rabbit anti-βIII-tubulin (1:3000, Covance), goat anti-Doublecortin (1:2000, Santa Cruz), goat anti-Brn3b (1:100, Santa Cruz), mouse anti-Brn3a (1:1000), mouse anti-Syntaxin (1:1000, Sigma), mouse anti-NF-160 (1:500, Sigma), mouse anti-Isl1 (1:20, DSHB), rabbit anti-Dlx (1:40), mouse anti-VC1.1 (1:400, Sigma), rabbit anti-Pax2 (1:1000, Covance), rabbit anti-Mitf (1:2000), sheep anti-Chx10 (1:1000, N terminal antisera, Exalpha Biologicals), rabbit anti-RXRγ (1:250, Santa Cruz), and rat anti-BrdU (1:100, Harlan/Serotec). Secondary antibodies were donkey anti-sheep-Alexa488 (1:1000), donkey anti-rat FITC (1:200), donkey anti-goat Texas Red (1:200), Cy2-goat anti-rabbit IgG (1:200), Cy3-donkey anti-mouse IgG (1:200), or donkey anti-rabbit biotin (1:200) followed by Streptavidin Texas Red (1:200). Labeled sections were imaged with a Leica fluorescent microscope and Orca camera or a Zeiss fluorescent microscope with a Zeiss camera and Apotome deconvolution device.

Cell counting

Neuron numbers were quantified from βIII-tubulin antibody labeling of serial 10-μm sections through the optic vesicles of Hes1+/+, +/−, and −/− embryos. Neuron counts were the average number of neurons ± SEM from a complete set of sections including both eyes of ≥3 embryos from each developmental age. Only strongly labeled cells were counted, with double counting of cells minimized as described in Philips et al. (2005).

BrdU (Sigma) injections and antibody labeling were performed in utero at E9.5 and E10.5 of development (Mastick and Andrews, 2001). At 1.5 h post-injection, embryos were collected, fixed, and processed for cryosectioning and antibody labeling. Wild type, *Hes1*+/−, and *Hes1*−/− embryonic heads were collected from three independent litters at E9.5 and E10.5. Equivalent optic sections were selected using anatomical landmarks in the embryonic head and counting serial sections. BrdU-labeled nuclei and total nuclei (DAPI labeled) were quantified for the surface ectoderm, optic vesicle, optic stalk, optic cup, or RPE. Two independent sections (separated by several sections) were analyzed for each genotype and age ($n \geq 3$ embryos). The labeling index (BrdU positive nuclei/DAPI labeled nuclei) was determined for each forming tissue of the E9.5 and E10.5 eye. These percentages were plotted and compared among genotypes using ANOVA and a Fisher test to determine *P* values.

Results

Comparison of Hes1 expression with other early eye genes

Hes1 mutant embryos have abnormal lenses and optic cups at E10.5 (Tomita et al., 1996a), suggesting that *Hes1* expression initiates prior to this age. Using whole-mount in situ hybridization, *Hes1* mRNA expression was examined from E7.5 through E10.5. *Hes1* expression was not observed in any region of the mouse embryo at E7.5. Beginning at E8.5, mRNA expression was observable within the anterior neural plate of 3-somite embryos (not shown). Expression was detected in slightly older (6-somite) embryos at the leading edge of the anterior neural plate (arrow in Fig. 1A) and in forming somites (not shown). As optic vesicle morphogenesis and neural tube closure proceeded, *Hes1* mRNA was apparent throughout the optic region (Fig. 1B). *Hes1* mRNA expression in the forming eye and brachial arches was quite prominent at E9.5 (Fig. 1C) and in the E10.5 optic cup (Fig. 1D). Because both the lens and optic cup form abnormally in *Hes1* mutants, we were interested to determine more precisely which cells express Hes1. A Hes1 polyclonal antisera was raised, affinity-purified, and its specificity verified by the lack of staining in *Hes1* mutants (Fig. 1F). During lens formation, Hes1 protein was observed at E8.5–E9.0 in the surface ectoderm (Fig. 1E), and at later ages in the lens placode and evaginating lens (Fig. 1G). Similarly, Hes1 protein is expressed in the optic vesicle, cup, stalk, and RPE, although not uniformly within the optic cup and RPE (Figs. 1E, G and data not shown).

In the optic vesicle, *Hes1* expression coincides with that of the eye specification genes *Rx* and *Pax6* (Koroma et al., 1997; Mathers et al., 1997; Walther and Gruss, 1991). To place *Hes1* function in context with other early eye genes, the molecular epistasis among four transcription factors was examined (Table 1). For this *Rx*, *Pax6*, *Hes1*, and *Math5* expression were compared between wild type and *Hes1* mutant littermates from E8.5 through E12.5 and integrated with what was previously reported (Brown et al., 1998; Zhang et al., 2000). Together, these data indicate that *Rx* is the most upstream since it is expressed normally in *Hes1* E9.5 mutant optic vesicles (n = 4/4 mutants), just as it is in *Pax6* and *Math5* mutants (Table 1). Likewise, *Pax6* expression is unaffected by loss of *Hes1* (n = 3/3 mutants) and *Math5* (n = 3/3 mutants) (Table 1). *Hes1* is upregulated in *Pax6* mutants, but only beginning at E10.5 (Brown et al., 1998), and unaffected by the loss of *Math5* (Table 1, n = 3/3 mutants). *Math5* is the most downstream, since its expression is affected in *Pax6* and *Hes1* mutants. Interestingly, *Math5* is downregulated by the removal of *Pax6* gene dosage but upregulated by the loss of *Hes1* (Figs. 4 and 6). These relationships correlate well with the mutant phenotype for each gene, namely, anophthalmia for *Rx*, microphthalmia for *Pax6* or *Hes1*, and specific loss of RGCs and optic nerves for *Math5* (Brown et al., 2001; Hill et al., 1991; Mathers et al., 1997; Tomita et al., 1996a; Wang et al., 2001).

Could the loss of *Hes1* cause optic vesicle repatterning that is manifested as arrested lens and optic cup formation? There are varying degrees of phenotypic severity in *Hes1* mutant embryos due to the mixed genetic background of these mice (see Materials and methods). In the eye, these phenotypes varied from a reduced lens accompanied by a smaller than normal optic cup (retina plus RPE) to the complete absence of the lens with an arrested optic vesicle. To understand the requirements for *Hes1* in the early eye better, we compared a

panel of eye markers between wild type and *Hes1*−/− eyes. *Pax2* is normally expressed throughout the optic vesicle and stalk at E9.5, but then becomes confined to the optic stalk at older ages (Nornes et al., 1990). No differences in Pax2 expression were observed between E9.5 wild type and *Hes1*−/− eyes (Figs. 2A, E; *n* = 3/3 embryos). Thus, the E10.5 *Hes1*−/− coloboma phenotype (failure of ventral optic cup and stalk to close, Tomita et al., 1996a) must arise downstream of *Pax2*. In addition, cryosections of late E9.5 optic vesicles were double labeled using antisera for the retinal marker Chx10 (Burmeister et al., 1996) and RPE marker Mitf (Steingrimsson et al., 1994; Tachibana et al., 1994). Both Chx10 and Mitf antibodies labeled distinct regions within the E9.5 and E10.5 *Hes1* mutant eye, implying that future retina (Chx10+ green cells in Figs. 2B, C) is specified and distinct from the forming RPE (Mitf+ red cells). Therefore, despite normal patterning, morphogenesis is arrested in severely affected mutant embryos (Fig. 2G; *n* = 3/3 mutant embryos). The earliest known optic cup marker, *Rx*, was also expressed normally in E10.5 *Hes1*−/− eyes despite the smaller size and abnormal morphology (Figs. 2D, H; *n* = 3/3 mutant embryos).

Next, we examined RPE formation more closely in *Hes1* mutants using *Mitf*, *Dct*, and *Tyrp1* expression. In E10.5 *Hes1*−/− eyes that underwent some morphogenesis, fewer *Mitf*+ RPE cells were observed (compare Figs. 2I, J with Figs. 2M, N; *n* = 4/4 mutant embryos). Likewise, *Dct* and *Tyrp1* expression domains, demarcating differentiated RPE (Kobayashi et al., 1998), were smaller at E10.5 (Figs 2K, O and data not shown; *n* = 2/2 mutants *Dct*, 3/3 mutants *Tyrp1*). *Dct* and *Tyrp1* expression was also assayed at E12.5 where they reflected small, abnormally formed RPE in *Hes1*−/− eyes (Figs. 2L, P; *n* = 3/3 mutant embryos for each marker). Although RPE tissue is reduced in *Hes1* mutants, differentiation appears spatiotemporally correct. We conclude that, despite the variable but highly abnormal morphogenesis of the lens, retina, and RPE, overall early eye patterning and specification is largely independent of *Hes1* function.

Hes1 is required for proliferation of the lens and optic stalk

In E10.5 *Hes1*−/− embryos, defects in the lens ranged from reduced size to its complete absence (Tomita et al., 1996a). We consistently observed that 50% of *Hes1*−/− embryos completely lacked a discernible lens, while the remainder exhibited a range of smaller than normal lenses with abnormal morphology (*n* > 25 litters). Initial lens specification must occur in *Hes1* mutants because we observed normal *Pax6* mRNA expression in the surface ectoderm and lens placode at E8.5–E10.5 (Table 1 and EW, NLB unpublished observations). Consistently, E10.5-E11.5 mutants had either an arrested optic vesicle or noticeably smaller optic cups. Together, these defects suggest that *Hes1* influences the proliferation of multiple eye tissues. To test this idea, E9.5 and E10.5 embryo litters (containing wild type, heterozygous, and homozygous mutants; *n* ≥ 3 embryos per age and genotype) were pulse-labeled with bromodeoxyuridine (BrdU) to identify cells in S-phase. Anti-BrdU and DAPI labeling of optic sections was used to quantify the percentage of S-phase cells in lens placode (lp), presumptive retina (pr), and RPE/optic stalk (Fig. 3). White lines in Figs. 3A – F indicate the boundaries assigned to each tissue. For all optic vesicles (normal to mutant E9.5 eyes or arrested E10.5 *Hes1* mutants), the forming optic stalk and RPE were grouped together. At E9.5, proliferation in the lens placode and presumptive

retina was unaffected by the loss of *Hes1* (Figs. 3C, E, and G). However, in *Hes1*+/− and *Hes1*−/− embryos, significantly fewer optic stalk/RPE S-phase cells were found (Fig. 3G).

At the outset, we predicted a loss of proliferation in the *Hes1*−/− retina since it is smaller than normal and exhibits premature neuronal differentiation. Instead, only a significant loss of lens proliferation was observed at E10.5 (Fig. 3G). At this age, lens cells exhibited a dosage-sensitivity to the loss of *Hes1*, in that *Hes1* heterozygotes also showed reduced lens proliferation (Figs. 3D, G). Interestingly, in *Hes1*+/− embryos, lens proliferation defects correlated with precocious and inappropriate neuron formation in the optic cup (Fig. 5). In cases where E10.5 mutants lacked a lens, S-phase cells were scored for the optic cup and RPE/OS but additional mutant embryos were analyzed to achieve equivalent lens sample sizes (Fig. 3F, $n = 6$ mutant litters). In conclusion, *Hes1* function is required for RPE/OS proliferation at E9.5 and lens proliferation at E10.5. These defects may underlie the altered morphology of the *Hes1* mutant eye.

Proneural bHLH expression is accelerated with unperturbed temporal order

Hes1 has been shown to repress retinal neuron development from E14.5 through P14 (Takatsuka et al., 2004; Tomita et al., 1996a). These experiments tested *Hes1* function in the retina after many retinal neurons had already differentiated. In these studies, the full extent of *Hes1* repression of retinal neurogenesis may be masked, because the presence of retinal neurons influences subsequent waves of neurogenesis. Indeed, Takatsuka et al. (2004) reported that, at E14.5, *Math5* mRNA is not upregulated in *Hes1* mutants although RGC genesis is clearly increased. In E10.5 *Hes1*−/− eyes, accelerated neurogenesis was demonstrated using a pan-neuronal marker (Tomita et al., 1996a). Therefore, how and to what extent *Hes1* represses the initiation of retinal neurogenesis remained largely undefined. To address this, we examined four retinal bHLH gene expression patterns (*Math5, Ngn2, NeuroD, Mash1*) in *Hes1* mutants prior to and at the initiation of retinogenesis (E8.5–E12.5). At E8.5, none of these proneural genes were expressed in the anterior neural plate or optic region of wild type, *Hes1*+/−, or *Hes1*−/− embryos ($n = 9$ litters). However, at E9.5, *Math5* was prematurely expressed in the optic vesicle of *Hes1* mutants, compared to wild type littermates (Figs. 4A–D, $n = 6/6$ mutant embryos). *Math5* expression was consistently observed in 22-somite mutant embryos but not at younger ages. The *Math5*-expressing cells were randomly arranged throughout the *Hes1*−/− optic vesicle (Figs. 4C inset, D), indicating a loss of the wild type dorso-central to peripheral activation pattern of *Math5* (Brown et al., 1998). Premature *Math5* expression was not detected in *Hes1* heterozygotes in whole-mount or sectioned embryos.

The removal of *Hes1* did not produce simultaneous upregulation of the four bHLH genes tested. Instead, the onset of *Math5, Ngn2,* and *Mash1* remained sequential. Differing phenotypes were observed regarding the timing of *Ngn2* and *Mash1* expression. First, *Ngn2* mRNA normally activates in the optic cup at E12.5 (HYL unpublished observations). E9.5 *Hes1* mutant optic vesicles were devoid of *Ngn2*-expressing cells (compare Figs. 4E, F and G, H), but *Ngn2* was prematurely expressed in the forming optic stalk (arrow, Fig. 4H; $n = 4/4$ embryos). Ectopic optic stalk expression was readily observable in sections of mutant embryos (compare Figs. 4H to F) and persisted through E11.5 (thick arrow, Fig. 4P). In the

E11.5 mutant optic cup, precocious activation of Ngn2 was clearly seen (Figs. 4O, P; *n* = 3/3 mutant embryos). Secondly, a small domain of *Mash1*-expressing cells is normally seen only in the dorsal optic vesicle at E9.5 (Guillemot and Joyner, 1993). In agreement with Ishibashi et al. (1995), we observed E10.5 *Hes1* homozygous mutants (but not heterozygotes) have an inappropriate *Mash1* domain (Figs. 4K, L) that disappeared by E11.5 (*n* = 3/3 mutants per age). Because the preponderance of *Mash1* expression occurs from E14.5 to P9 in retinal progenitors (Jasoni and Reh, 1996), the significance of the E9.5 domain and its persistence for an extra day in *Hes1* mutants is unclear. By contrast, we found normal spatial and temporal expression of *NeuroD* in E9.5 to E12.5 *Hes1* mutants (*n* ≥ 3 litters at each age; not shown). Thus, the absence of *Hes1* results in precocious activation rather than an overall increase in the number of retinal progenitors expressing proneural genes. Intriguingly, the loss of *Hes1* did not perturb the sequence of proneural gene activation (*Math5* ⇒ *Ngn2* ⇒ *Mash1*).

Precocious Hes1−/− retinal neurons express RGC, amacrine, and horizontal markers

Math5, *Ngn2*, and (to a lesser degree) *Mash1* are prematurely expressed in *Hes1* mutant eyes; hence, it was important to determine the earliest time of precocious neuronal differentiation. For this, we examined the neuron-specific marker βIII-tubulin in E9–E11 *Hes1* mutant litters (Fig. 5). No expression of βIII-tubulin was observed in wild type embryos at E9.5 or E10.5 (Figs. 5A, D). In *Hes1* mutants, many optic cells express βIII-tubulin beginning at E9.5 (Figs. 5C, F). We also observed small numbers of optic vesicle or cup cells expressing βIII-tubulin in *Hes1* heterozygotes (arrows in Figs. 5B, E). Numerous labeled cells had differentiated neuronal morphology with extended neurites (arrow in Fig. 5C). βIII-tubulin-expressing cells were quantified in serial sections through the optic region of somite-matched wild type, *Hes1*+/−, and *Hes1*−/− embryos at E9.5 and E10.5. At each age, the total number of βIII-tubulin-expressing cells in the optic vesicle or cup of both eyes was quantified: E9.5 (24–26 somites): wild type = 0 ± 0 (*n* = 3 embryos), *Hes1*+/− = 1.8 ± 1.4 (*n* = 4 embryos) and *Hes1*−/− = 213 ± 56.5 (*n* = 3 embryos); E10.5 (33–36 somites): wild type = 0 ± 0 (*n* = 5 embryos), *Hes1*+/− = 4.8 ± 2.5 (*n* = 4 embryos) and *Hes1*−/− = 222 ± 6.0 (*n* = 3 embryos). Thus, *Hes1* mutant optic vesicle cells undergo neuronal differentiation at earlier ages than previously reported (Ishibashi et al., 1995).

To determine if mutant optic cup neurons adopt particular fates, we tested eight different markers of RGC, amacrine, or horizontal differentiation in double-label experiments with βIII-tubulin at E9.5 and E10.5. In no case was there a 1:1 correlation between the marker of interest and βIII-tubulin. Instead, a portion of βIII-tubulin cells co-labeled with Doublecortin (Fig. 5G), NF160 (Fig. 5H), Brn3a (Fig. 5J), Brn3b (Fig. 5K), or Isl1 (Fig. 5L). In wild type, each of these markers exhibits RGC-specific expression during prenatal mouse retinal development (Brown et al., 2001; Galli-Resta et al., 1997; Nixon et al., 1989; Rachel et al., 2002; Trieu et al., 2003; Xiang et al., 1993). One progenitor marker, Dlx, was completely lacking in *Hes1*−/− eyes (Fig. 5M), despite robust expression in a subset of cells in the wild type optic cup. The pan-Dlx antibody used (Panganiban et al., 1995) probably recognizes Dlx1 and Dlx2, two proteins that are expressed by prenatal mouse retinal progenitors and early-born neurons (Eisenstat et al., 1999), implying that *Hes1*−/− eyes lack Dlx activation.

Many βIII tubulin-positive, *Hes1*−/− optic cup cells adopt RGC fates since they express Brn3a, Brn3b, NF160, Doublecortin, or Isl1.

Because amacrine and horizontal neurons prematurely differentiate in *Hes1*−/− postnatal retinae (Tomita et al., 1996a), we tested two markers, Syntaxin (Barnstable et al., 1985) and VC1.1, which detect these cell types. Rodent amacrine cells express VC1.1 slightly earlier than Syntaxin (Alexiades and Cepko, 1997). While Syntaxin is expressed by nearly all amacrine neurons, no expression was found in *Hes1* mutant optic cups (Fig. 5I). Both amacrine and horizontal neurons normally express VC1.1 (Alexiades and Cepko, 1997; Arimatsu et al., 1987) and we detected expression in E9.5 (not shown) and E10.5 mutants (Fig. 5N). Most precocious VC1.1-expressing cells did not also express βIII tubulin (red only cells in Fig. 5N). Because βIII tubulin expression is better described during horizontal neuron differentiation than it is for amacrines (Brittis and Silver, 1994; Brown et al., 2001; Watanabe et al., 1991), we interpret this to mean that VC1.1 single-labeled cells adopt amacrine characteristics while the smaller number of double-labeled cells may be horizontal neurons (arrow in Fig. 5N). Alternatively, the VC1.1 single-labeled cohort may be immature horizontal neurons. The other early retinal neuron class, cone photoreceptors, was assessed using the cone marker RXRγ (Mori et al., 2001). By this criterion, precocious cones were not detected in *Hes1* mutants at either E9.5 or E10.5.

Hes1 and Pax6 regulation of Math5

Although coinjection of activated Notch and Pax6 appears to synergistically promote *Xenopus* ectopic eye formation (Onuma et al., 2002), genetic interactions between *Hes1* and *Pax6* have not been formally tested in vertebrates. Therefore, we explored this idea since both genes are expressed in the early eye, multiple eye tissues are affected in *Hes1* and *Pax6* mutants and *Hes1* expression is upregulated at E10.5 in *Pax6*−/− embryos (Brown et al., 1998). Because *Math5* expression is oppositely affected in *Pax6* and *Hes1* mutants, it was used to test for epistasis. If *Math5* expression is precocious or its domain expanded in *Hes1*−/−;*Pax6*−/− double mutants, it would indicate that *Hes1* regulates *Math5* genetically downstream from *Pax6*. A mouse strain with one copy each of the *Hes1* targeted deletion and *Pax6-Sey*^{Neu1} null mutation was created. These mice were intercrossed and the varying dosages of each mutation determined by PCR genotyping of embryonic tail tissue. *Math5* mRNA was assayed by in situ hybridization in E11.5 embryos. The *Math5* expression domain diminished as the dosage of *Pax6* decreased (Brown et al., 1998, Figs. 6A, E, and I), irrespective of *Hes1* gene dosage (Figs. 6C, G, and K). Additionally, the *Math5* domain expanded in embryos that completely lack *Hes1* (compare Figs. 6C, D to Figs. 6A, B). In *Pax6* heterozygotes, increasing numbers of Math5-expressing cells correlated with decreased dosage of *Hes1* (compare Figs. 6G to E). However there were fewer *Math5*-positive cells than when *Pax6* gene dosage is normal (Figs. 6C, D). Thus, while *Pax6* is necessary for *Math5* activation and *Hes1* for *Math5* repression, each gene independently regulates *Math5*. This implies that *Pax6* does not act through *Hes1* to regulate *Math5* expression but, likely controls *Math5* transcription directly, as proposed by Marquardt et al. (2001).

Hes1 and Pax6 interaction during optic vesicle morphogenesis

In *Pax6* mutants, morphogenesis initiates but arrests at the optic vesicle stage and the lens is not induced (Fig. 6J and Grindley et al., 1995; Hill et al., 1991; Hogan et al., 1986). *Hes1* mutant morphology is largely identical to *Pax6* mutants (Tomita et al., 1996a). Although *Pax6* and *Hes1* regulate retinal neurogenesis via *Math5* expression separately, it is plausible that they may have similar or overlapping functions in optic vesicle morphogenesis. In support of this, *Pax6−/−;Hes1−/−* embryos lack an eye at E11.5 (Figs. 6K, L). No remnants of lens or optic vesicle/cup were detected in serial sections of double mutant embryos, although a small protrusion of the diencephalon neural tube was observed (arrows in Fig. 6L). In addition, *Pax6+/−;Hes1−/−* embryos had more extreme defects to the optic cup and lens (Fig. 6H) than either single mutant alone or double heterozygotes. Finally, *Pax6+/−;Hes1+/−* optic cups (Fig. 6F) are malformed with reduced lens compared to wild type siblings (Fig. 6B) or *Pax6*+/− embryos (Brown et al., 1998).

The dramatic loss of the optic vesicle in Pax6−/−Hes1−/− eyes was unanticipated. To determine how early this occurs, serial sections of embryos from E9.5 *Pax6+/−Hes1+/−* crosses were examined. An evaginated optic vesicle and thickened lens placode are easily recognized in wild type embryos (Figs. 7A, F, and K). In either *Pax6−/−* and *Hes1−/−* single mutant embryos, an optic vesicle was distinguishable at gross and histologic levels by its anatomical position and morphology (Figs. 7B, C, G, and H). *Pax6−/−;Hes1−/−* double mutants lack these structures grossly (Fig. 7M) and in cross section. In only one to two 10-μm sections could a rudimentary evagination of the neural tube be found (Figs. 7D, E, I, and J; *n* = 3/3 embryos). Severe forebrain morphologic defects were also apparent.

The failure of the double mutant optic tissue to evaginate could arise either from a failure to specify the early eye field, or by a defect in normal morphogenetic outgrowth of specified eye tissue. To distinguish between these possibilities, mRNA expression of a very early marker for the eye field, *Rx*, was examined in E9.5 embryo litters from *Pax6+/−;Hes1+/−* matings (Figs. 7L, N and data not shown, *n* = 11 litters). Within the presumptive eye area of double mutants, corresponding to where the protrusion was seen in sections, we observed *Rx* mRNA expression (Figs. 7J, N; 4/4 double mutant embryos). This suggests that the eye field is specified independently, but overt optic vesicle outgrowth is dependent on the combined functions of *Hes1* and *Pax6*. From this, we conclude that *Hes1* and *Pax6* interact cooperatively, downstream of *Rx*, to regulate optic vesicle morphogenesis.

Discussion

Hes1 in lens and optic vesicle formation

The growth and morphogenesis of the lens and optic cup are two key early events in the vertebrate eye. Initial characterization of the *Hes1* targeted deletion indicated that these processes and tissues may require *Hes1* (Tomita et al., 1996a). Here, we show that every part of the early eye expresses *Hes1* and loss of *Hes1* predominantly affects lens, optic cup, and RPE development. To understand the optic cup phenotype better, we examined five early ocular markers, *Rx*, *Pax6*, *Pax2*, *Mitf*, and *Chx10*. Together, their expression indicates that the future retina is specified and basically patterned in the absence of *Hes1*, yet *Hes1−/−*

optic vesicles fail to progress into a cup shape. It is plausible that the reduction or total absence of the lens influences *Hes1*−/− optic vesicle morphogenesis. But it also raises the circular argument that *Hes1* may act simultaneously in both the lens and optic vesicle (similar to *Pax6*). However, some defects could be indirectly due to disrupted signaling between these two tissues. The conundrum of which tissue, the lens or the optic vesicle, requires *Hes1* can only be addressed by determining the cell autonomy of each early mutant phenotype. A similar evaluation of *Notch* pathway components should also be undertaken to demonstrate which *Hes1* functions arise from *Notch* signaling.

Hes1 and RPE differentiation

Interestingly, loss of *Hes1* function caused a reduction in RPE tissue. This phenotype is similar to *Pax6/Pax2* double mutants that display reduced *Mitf* expression (Baumer et al., 2003). In this case, the loss of RPE arises from its transdetermination into retina. We did not find evidence for this in *Hes1* mutants in that neither *Rx* nor *Chx10* was inappropriately expressed in the forming RPE, although some *Hes1*−/− RPE cells ectopically express βIII tubulin (Fig. 5). Since *Hes1* genetically interacts with *Pax6*, it might be a downstream component of *Pax* gene regulation of *Mitf* for the RPE. However, Pax6 and Pax2 bind to the *Mitf-A* promoter in vitro to direct the transcriptional activation of a particular Mitf isoform (Baumer et al., 2003). *Mitf* regulation is complicated by its multiple promoters, and activation by *Pax6* and *Pax2* is unlikely to account for all *Mitf* activity in the early eye. It is possible that Hes1 binds to the same or a different *Mitf* promoter. We do not favor this possibility because *Hes1* acts as a repressor and *Mitf* expression is reduced, not increased, in *Hes1* mutants. Thus, a direct role for *Hes1* in RPE development likely involves additional factors. The function of *Hes1* in the RPE can be deciphered further by testing for its cell autonomous requirement and investigating ectopic *Ngn2* expression and neuron formation in the E9.5 optic stalk/RPE. Together, this should establish whether there is a direct regulatory role for *Hes1* in RPE differentiation or it indirectly regulates the RPE via the optic vesicle/cup.

Hes1 as a temporal repressor of neurogenesis

We propose that *Hes1* is a temporal brake that integrates the timing of neurogenesis with morphogenesis. Importantly, we did not observe simultaneous acceleration of four bHLH genes *in Hes1* mutants. Instead, the order of *Math5, Ngn2*, and *Mash1* activation was unperturbed, yet initial activation of each was temporally advanced. Likewise, the timing of early retinal neuron markers remained generally intact. Paradoxically, *NeuroD*, the amacrine-promoting factor, was not expressed precociously, but one early amacrine marker, VC1.1, was accelerated in *Hes1* mutants. Because we observed VC1.1, but not Syntaxin expression, it is possible that some or all of the precocious neurons are incompletely differentiated. Additionally, the loss of *Hes1* does not cause global derepression of retinal neurogenesis since precocious bHLH and neuronal markers were undetectable prior to the 22-somite age in *Hes1* mutant optic vesicles (HYL and EW unpublished observations). This might suggest that very young optic cells are unable to differentiate. Although their neural competence was not directly tested, *Hes1* is normally expressed throughout the forming optic region much earlier than this stage, yet its genetic removal did not promote accelerated neurogenesis before a particular developmental time point.

Recently, the optic vesicles of embryos completely null for *Pax6* were found to contain precocious neurons (Philips et al., 2005). However, *Hes1* neuronal phenotypes differ from those of *Pax6* mutants in two important ways. First, the early optic cup mutations in either *Hes1* or *Pax6* accelerate neuron formation, yet *Pax6*−/− neurons are unable to choose a retinal fate. Secondly, retinal-specific *Pax6* mutations abolish proneural expression and the production of all retinal classes, except for *NeuroD* expression and amacrines (Marquardt et al., 2001). Consequently, it will be important to determine if *Hes1* regulates the timing of amacrine differentiation independent of *NeuroD*. Because *Math3* and *Six3* positively influence amacrine fate (Inoue et al., 2002), *Hes1* mutants may normally suppress either gene to block amacrine differentiation independent of *NeuroD*.

Notch-dependent and -independent functions of Hes1

The *Notch* pathway regulates distinct aspects of retinal neurogenesis (Ahmad et al., 1997; Austin et al., 1995; Dorsky et al., 1995, 1997; Henrique et al., 1997; Schneider et al., 2001). In the chick retina, constitutively active or dominant negative forms of *Delta* influence RGC, cone, or amacrine fates (Ahmad et al., 1997; Henrique et al., 1997). However, little is known about the role of *Notch* signaling during vertebrate eye induction, morphogenesis, and patterning, particularly if it drives *Hes1* repressor activity. In the fly eye, *Notch* signaling is integral to photoreceptor development (Baker, 2000; Baonza and Freeman, 2001). Mammalian *Hes1* is homologous to both *Drosophila hairy* and *Enhancer of split* and behaves in particular contexts as a downstream effector of *Notch* signaling. For example, constitutively active Notch upregulates a *Hes1* promoter in cultured cells (Jarriault et al., 1995, 1998). This activity requires RBP-Jx binding to the *Hes1* promoter (Jarriault et al., 1995). In the rodent retina, *Notch1* and *Hes1* are both expressed in Mu¨ller glia and promote their formation (Bao and Cepko, 1997; Furukawa et al., 2000). The Notch ligand Delta was reported to trigger *Hes1* mRNA oscillation in vitro (Hirata et al., 2002) and in the presomitic mesoderm, periodic *Hes1* expression follows periodic *fringe-Notch* signaling (Dale and Maroto, 2003; Dubrulle and Pourquie, 2002). Therefore, in particular contexts, *Hes1* responds to *Notch*. But it is unclear whether *Hes1* is completely *Notch-dependent* since its expression is normal in *Notch1* and *RBP-Jx* mutant embryos (de la Pompa et al., 1997). It is plausible that *Hes1* is *Notch*-dependent in the somite, but able to act independently in the early optic vesicle.

Instead, we favor the idea that *Hes1* responds to *Notch* in particular developmental processes such as lateral inhibition and Mu¨ller glial differentiation, but might act independent from *Notch* during early morphogenesis (where it genetically interacts with *Pax6*). The ability of *Xhairy2* to function independent of *Notch* in the frog anterior neural plate supports this idea (Andreazzoli et al., 2003). However, optic vesicle morphogenesis also fails in *Hes1–Hes5* double mutants (Hatakeyama et al., 2004). This eyeless phenotype may arise differently since *Chx10* and *Pax2* mRNA are not expressed in *Hes1*−/−*Hes5*−/− mutants (Hatakeyama et al., 2004), while Chx10 and Pax2 are normal in *Hes1*−/− optic vesicles (Fig. 2). Therefore, *Chx10* and *Pax2* may be downstream *of Notch* signaling that is completely removed in *Hes1–Hes5* double mutants. To understand the requirements for *Notch* and its pathway components during early eye formation, each gene's regulation of *Chx10* and *Pax2* should be tested directly.

How does *Hes1* act as a temporal regulator? Molecularly, *Hes1* repression is complicated since it can either inhibit neurogenesis through promoter binding (Sasai et al., 1992; Takebayashi et al., 1994) or form inactive heterodimers with proneural proteins (Ohsako et al., 1994). Regulation of *Hes1* expression is similarly multifaceted and minimally includes oscillating *Hes1* mRNA and protein expression and rapid Hes1 protein turnover via ubiquitination (Hirata et al., 2002). It is plausible that multiple molecular mechanisms are at work in the developing mammalian eye, allowing Hes1 to precisely orchestrate distinct cellular processes. Alternatively, the different modes of *Hes1* regulation and action might be tissue-specific. Consistent with this idea, activation of *Hes1* is downstream of *Rx/Rax* in the postnatal retina (Furukawa et al., 2000). Thus, *Hes1* may exhibit different functions throughout the body via its regulation by tissue-restricted factors. To clarify these ideas, it will be important to define mechanisms of *Hes1* mRNA and protein regulation in the eye and to what extent *Notch* signaling is involved.

The actions of Hes1 and Pax6 in multiple stages of eye development

Hes1 and *Pax6* genetically interact, which is demonstrated by the temporal sensitivity of *Hes1* expression to *Pax6* gene dosage beginning in the E10.5 optic cup (Brown et al., 1998). Paradoxically, in younger optic vesicles, *Hes1* is unaffected by the loss of *Pax6* (Table 1). Therefore, we did not predict that double mutant embryos would be unable to undergo optic vesicle morphogenesis. Because *either Pax6* or *Hes1* is sufficient for the initiation of vesicle formation, it suggests that these two genes have overlapping functions for morphogenesis. One plausible mechanism through which *Pax6* and *Hes1* could synergize is that while both single mutants have reduced proliferation, either gene is sufficient to promote the amount of proliferation needed for vesicle formation. In double mutants, little to no proliferation occurs such that vesicle initiation is blocked. Alternatively, *Pax6* and *Hes1* may regulate or interact with another early eye transcription factor, *Lhx2*, since embryos mutant for this gene exhibit anophthalmia, similar to the *Pax6–Hes1* double mutants (Porter et al., 1997). Overall, the mechanisms for eye morphogenesis remain mysterious, but clearly *Hes1* and *Pax6* play key roles in this process.

There may also be two separable periods for *Pax6* and *Hes1* interaction. The first is during optic vesicle and lens morphogenesis, while the second is the initiation of retinal neurogenesis via transcription of *Math5*. At the earliest stages, *Pax6* and *Hes1* might interact during reciprocal induction of the lens and optic vesicle or during RPE specification. Because so little is known about the molecular mechanisms of eye morphogenesis, it is not yet possible to invoke one for *Pax6* and *Hes1* interaction, except that it occurs parallel to or downstream of eye field specification. However, for RGC neurogenesis, Pax6 and Hes1 act in opposite and independent manners. The simplest model for this employs *Pax6* transcriptional activation of *Math5* that is balanced by *Hes1* transcriptional repression. These inputs might be maintained stoichiometrically and/or through temporally offset binding to a *Math5* enhancer element. For example, the presence of *Pax6*, beginning in the optic vesicle and continuing in the cup and retina, appears sufficient for *Math5* transcription. However, when high levels of *Hes1* are present at E9.5–E10.5, *Math5* transcription is silent. As *Hes1* levels decline sufficiently, *Math5* mRNA appears in the dorso-central cup at E11.

An emerging paradigm of developmental neurobiology is the combinatorial action of homeobox and bHLH transcription factors in the specification of particular types of neurons (Cau et al., 2002; Hatakeyama et al., 2001; Isshiki et al., 2001; Yun et al., 2002). *Pax6* and *Hes1* regulate the timing of retinal neurogenesis, although in each case the specification of precocious neurons differs. This might be explained through the opposing modes of transcriptional regulation (activation versus repression). Unexpectedly, at early stages of eye formation, the presence of both genes is critically required for optic morphogenesis. This suggests that the combined functions of homeobox and bHLH proteins must also include potential combinations of transcriptional activators and repressors, with broader roles that include morphogenesis.

Acknowledgments

The authors thank Jane Johnson for *Hes1* mutant mice, Grace Boekhoff-Falk for Dlx antibody, Eric Turner for Brn3a antibody, Heinz Arnheiter and Leigh-Ann Miller for Mitf antibody, Tom Glaser and Colin Hodgkinson for *Rx* and *Mitf* cDNAs, D. Jonathan Horsford for Dct and Tyrp1 cDNAs, Bill Goossens and April Smith for assistance with imaging, and Tien Le for technical assistance. We also thank Kenny Campbell and Richard Lang for valuable discussions; and Steve Easter and Kenny Campbell for critical reading of the manuscript. This work was supported by NIH grants R01 HD38069 (GSM), R01 EY13612 (NLB), undergraduate fellowships from the Nevada Biomedical Research Infrastructure Network (CNS), and undergraduate research grants from the University of Nevada VP for Research (GTP and CNS).

References

Ahmad I, Dooley CM, Polk DL. Delta-1 is a regulator of neurogenesis in the vertebrate retina. Dev. Biol. 1997; 185:92–103. [PubMed: 9169053]

Akagi T, Inoue T, Miyoshi G, Bessho Y, Takahashi M, Lee JE, Guillemot F, Kageyama R. Requirement of multiple basic helix-loop-helix genes for retinal neuronal subtype specification. J. Biol. Chem. 2004; 279:28492–28498. [PubMed: 15105417]

Alexiades MR, Cepko CL. Subsets of retinal progenitors display temporally regulated and distinct biases in the fates of their progeny. Development. 1997; 124:1119–1131. [PubMed: 9102299]

Andreazzoli M, Gestri G, Cremisi F, Casarosa S, Dawid IB, Barsacchi G. Xrx1 controls proliferation and neurogenesis in *Xenopus* anterior neural plate. Development. 2003; 130:5143–5155. [PubMed: 12975341]

Arimatsu Y, Naegele JR, Barnstable CJ. Molecular markers of neuronal subpopulations in layers 4, 5, and 6 of cat primary visual cortex. J. Neurosci. 1987; 7:1250–1263. [PubMed: 3553447]

Austin CP, Feldman DE, Ida JA, Cepko CL. Vertebrate retinal ganglion cells are selected from competent progenitors by the action of *Notch*. Development. 1995; 121:3637–3650. [PubMed: 8582277]

Baker NE. Notch signaling in the nervous system. Pieces still missing from the puzzle. Bioessays. 2000; 22:264–273. [PubMed: 10684586]

Bao ZZ, Cepko CL. The expression and function of Notch pathway genes in the developing rat eye. J. Neurosci. 1997; 17:1425–1434. [PubMed: 9006984]

Baonza A, Freeman M. Notch signalling and the initiation of neural development in the *Drosophila* eye. Development. 2001; 128:3889–3898. [PubMed: 11641214]

Barnstable CJ, Hofstein R, Akagawa K. A marker of early amacrine cell development in rat retina. Brain Res. 1985; 352:286–290. [PubMed: 3896407]

Baumer N, Marquardt T, Stoykova A, Spieler D, Treichel D, Ashery-Padan R, Gruss P. Retinal pigmented epithelium determination requires the redundant activities of Pax2 and Pax6. Development. 2003; 130:2903–2915. [PubMed: 12756174]

Brittis PA, Silver J. Exogenous glycosaminoglycans induce complete inversion of retinal ganglion cell bodies and their axons within the retinal neuroepithelium. Proc. Natl. Acad. Sci. U. S. A. 1994; 91:7539–7542. [PubMed: 8052616]

Brown NL, Kanekar S, Vetter ML, Tucker PK, Gemza DL, Glaser T. Math5 encodes a murine basic helix-loop-helix transcription factor expressed during early stages of retinal neurogenesis. Development. 1998; 125:4821–4833. [PubMed: 9806930]

Brown NL, Patel S, Brzezinski JA, Glaser T. Math5 is required for retinal ganglion cell and optic nerve development. Development. 2001; 128:2497–2508. [PubMed: 11493566]

Burmeister M, Novak J, Liang MY, Basu S, Ploder L, Hawes NL, Vidgen D, Hoover F, Goldman D, Kalnins VI, et al. Ocular retardation mouse caused by Chx10 homeobox null allele: impaired retinal progenitor proliferation and bipolar cell differentiation. Nat. Genet. 1996; 12:376–384. [PubMed: 8630490]

Cau E, Gradwohl G, Casarosa S, Kageyama R, Guillemot F. Hes genes regulate sequential stages of neurogenesis in the olfactory epithelium. Development. 2000; 127:2323–2332. [PubMed: 10804175]

Cau E, Casarosa S, Guillemot F. Mash1 and Ngn1 control distinct steps of determination and differentiation in the olfactory sensory neuron lineage. Development. 2002; 129:1871–1880. [PubMed: 11934853]

Chen CM, Cepko CL. Expression of Chx10 and Chx10-1 in the developing chicken retina. Mech. Dev. 2000; 90:293–297. [PubMed: 10640715]

Dale JK, Maroto M. A Hes1-based oscillator in cultured cells and its potential implications for the segmentation clock. Bioessays. 2003; 25:200–203. [PubMed: 12596223]

Davis R, Turner DL. Vertebrate hairy and Enhancer of split related proteins: transcriptional repressor regulating celluar differentiation and embryonic patterning. Oncogene. 2001; 20:8342–8357. [PubMed: 11840327]

de la Pompa JL, Wakeham A, Correia KM, Samper E, Brown S, Aguilera RJ, Kakano T, Honjo T, Mak TW, Rossant J, et al. Conservation of the Notch signaling pathway in mammalian neurogenesis. Development. 1997; 124:1139–1148. [PubMed: 9102301]

Dorsky RI, Rapaport DH, Harris WA. *Xotch* inhibits cell differentiation in the *Xenopus* retina. Neuron. 1995; 14:487–496. [PubMed: 7695895]

Dorsky RI, Chang WS, Rapaport DH, Harris WA. Regulation of neuronal diversity in the *Xenopus* retina by Delta signalling. Nature. 1997; 385:67–70. [PubMed: 8985247]

Dubrulle J, Pourquie O. From head to tail: links between the segmentation clock and antero-posterior patterning of the embryo. Curr. Opin. Genet. Dev. 2002; 12:519–523. [PubMed: 12200156]

Eisenstat DD, Liu JK, Mione M, Zhong W, Yu G, Anderson SA, Ghattas I, Puelles L, Rubenstein JL. DLX-1, DLX-2, and DLX-5 expression define distinct stages of basal forebrain differentiation. J. Comp. Neurol. 1999; 414:217–237. [PubMed: 10516593]

Furukawa T, Kozak CA, Cepko CL. *rax*, a novel paired-type homeobox gene, shows expression in the anterior neural fold and developing retina. Proc. Natl. Acad. Sci. 1997; 94:3088–3093. [PubMed: 9096350]

Furukawa T, Mukherjee S, Bao ZZ, Morrow EM, Cepko CL. rax, Hes1, and notch1 promote the formation of Muller glia by postnatal retinal progenitor cells. Neuron. 2000; 26:383–394. [PubMed: 10839357]

Galli-Resta L, Resta G, Tan SS, Reese BE. Mosaics of islet-1-expressing amacrine cells assembled by short-range cellular interactions. J. Neurosci. 1997; 17:7831–7838. [PubMed: 9315903]

Grindley JC, Davidson DR, Hill RE. The role of Pax-6 in eye and nasal development. Development. 1995; 121:1433–1442. [PubMed: 7789273]

Guillemot F, Joyner AL. Dynamic expression of the murine Achaete-Scute homologue Mash-1 in the developing nervous system. Mech. Dev. 1993; 42:171–185. [PubMed: 8217843]

Hargrave, M.; Koopman, P. In situ hybridization of whole mouse embryos. In: Darby, I., editor. In Situ Hybridization Protocols. Vol. 123. Humana Press; Totowa, NJ: 2000. p. 279-289.

Hatakeyama J, Tomita K, Inoue T, Kageyama R. Roles of homeobox and bHLH genes in specification of a retinal cell type. Development. 2001; 128:1313–1322. [PubMed: 11262232]

Hatakeyama J, Bessho Y, Katoh K, Ookawara S, Fujioka M, Guillemot F, Kageyama R. Hes genes regulate size, shape and histogenesis of the nervous system by control of the timing of neural stem cell differentiation. Development. 2004; 131:5539–5550. [PubMed: 15496443]

Henrique D, Hirsinger E, Adam J, Le Roux I, Pourquie O, Ish-Horowicz D, Lewis J. Maintenance of neuroepithelial progenitor cells by Delta-Notch signalling in the embryonic chick retina. Curr. Biol. 1997; 7:661–670. [PubMed: 9285721]

Hill RE, Favor J, Hogan BLM, Ton CCT, Saunders GF, Hanson IM, Prosser J, Jordan T, Hastie ND, van Heyningen V. Mouse *Small eye* results from mutations in a paired-like homeobox-containing gene. Nature. 1991; 354:522–525. [PubMed: 1684639]

Hinds JW, Hinds PL. Early ganglion cell differentiation in the mouse retina: an electron microscopic analysis utilizing serial sections. Dev. Biol. 1974; 37:381–416. [PubMed: 4826283]

Hirata H, Yoshiura S, Ohtsuka T, Bessho Y, Harada T, Yoshikawa K, Kageyama R. Oscillatory expression of the bHLH factor Hes1 regulated by a negative feedback loop. Science. 2002; 298:840–843. [PubMed: 12399594]

Hogan BLM, Horsburgh G, Cohen J, Hetherington CM, Fisher G, Lyon MF. *Small eyes* (*Sey*): a homozygous lethal mutation on chromosome 2 which affects the differentiation of both lens and nasal placodes in the mouse. J. Embryol. Exp. Morphol. 1986; 97:95–110. [PubMed: 3794606]

Holt CE, Bertsch TW, Ellis HM, Harris WA. Cell determination in the *Xenopus* retina is independent of lineage and birth date. Neuron. 1988; 1:15–26. [PubMed: 3272153]

Inoue T, Hojo M, Bessho Y, Tano Y, Lee JE, Kageyama R. Math3 and NeuroD regulate amacrine cell fate specification in the retina. Development. 2002; 129:831–842. [PubMed: 11861467]

Ishibashi M, Moriyoshi K, Sasai Y, Shiota K, Nakanishi S, Kageyama R. Persistent expression of helix-loop-helix factor HES-1 prevents mammalian neural differentiation in the central nervous system. EMBO J. 1994; 13:1799–1805. [PubMed: 7909512]

Ishibashi M, Ang S-L, Shiota K, Nakanishi S, Kageyama R, Guillemot F. Targeted disruption of mammalian hairy and Enhancer of split homolog-1 (HES-1) leads to up-regulation of neural helix-loop-helix factors, premature neurogenesis, and severe neural tube defects. Genes Dev. 1995; 9:9136–9148.

Isshiki T, Pearson B, Holbrook S, Doe CQ. *Drosophila* neuroblasts sequentially express transcription factors which specify the temporal identity of their neuronal progeny. Cell. 2001; 106:511–521. [PubMed: 11525736]

Jarriault S, Brou C, Logeat F, Schroeter EH, Kopan R, Israel A. Signalling downstream of activated mammalian Notch. Nature. 1995; 377:355–358. [PubMed: 7566092]

Jarriault S, Le Bail O, Hirsinger E, Pourquie O, Logeat F, Strong CF, Brou C, Seidah N, Israel A. Delta-1 activation of Notch-1 signaling results in HES-1 transactivation. Mol. Cell. Biol. 1998; 18:7423–7431. [PubMed: 9819428]

Jasoni C, Reh T. Temporal and spatial pattern of MASH-1 expression in the developing rat retina demonstrates progenitor cell heterogeneity. J. Comp. Neurol. 1996; 369:319–327. [PubMed: 8727003]

Kageyama R, Ohtsuka T, Tomita K. The bHLH gene Hes1 regulates differentiation of multiple cell types. Mol. Cells. 2000; 10:1–7.

Kobayashi T, Imokawa G, Bennett DC, Hearing VJ. Tyrosinase stabilization by Tyrp1 (the brown locus protein). J. Biol. Chem. 1998; 273:31801–31805. [PubMed: 9822646]

Koroma BM, Yang JM, Sundin OH. The Pax-6 homeobox gene is expressed throughout the corneal and conjunctival epithelia. Invest. Ophthalmol. Visual Sci. 1997; 38:108–120.

Liu W, Mo Z, Xiang M. The Ath5 proneural genes function upstream of Brn3 POU domain transcription factor genes to promote retinal ganglion cell development. Proc. Natl. Acad. Sci. U. S. A. 2001; 98:1649–1654. [PubMed: 11172005]

Livesey FJ, Cepko CL. Vertebrate neural cell-fate determination: lesson from the retina. Nat. Rev. 2001; 2:109–118.

Marquardt T, Ashery-Padan R, Andrejewski N, Scardigli R, Guillemot F, Gruss P. Pax6 is required for the multipotent state of retinal progenitor cells. Cell. 2001; 105:43–55. [PubMed: 11301001]

Mastick GS, Andrews GL. Pax6 regulates the identity of embryonic diencephalic neurons. Mol. Cell. Neurosci. 2001; 17:190–207. [PubMed: 11161479]

Mathers PH, Grinbery A, Mahon KA, Jamrich M. The Rx homoeobox gene is essential for vertebrate eye development. Nature. 1997; 387:603–607. [PubMed: 9177348]

Mori M, Ghyselinck NB, Chambon P, Mark M. Systematic immunolocalization of retinoid receptors in developing and adult mouse eyes. Invest. Ophthalmol. Visual Sci. 2001; 42:1312–1318. [PubMed: 11328745]

Morrow EM, Furukawa T, Lee JE, Cepko CL. NeuroD regulates multiple functions in the developing neural retina in rodent. Development. 1999; 126:23–36. [PubMed: 9834183]

Nixon RA, Lewis SE, Dahl D, Marotta CA, Drager UC. Early posttranslational modifications of the three neurofilament subunits in mouse retinal ganglion cells: neuronal sites and time course in relation to subunit polymerization and axonal transport. Brain Res. Mol. Brain Res. 1989; 5:93–108. [PubMed: 2469928]

Nornes HO, Dressler GR, Knapik EW, Deutsch U, Gruss P. Spatially and temporally restricted expression of Pax2 during murine neurogenesis. Development. 1990; 109:797–809. [PubMed: 1977575]

Ohsako S, Hyer J, Panganiban G, Oliver I, Caudy M. *hairy* function as a DNA-binding HLH repressor of *Drosophila* sensory organ formation. Genes Dev. 1994; 8:2743–2755. [PubMed: 7958930]

Onuma Y, Takahashi S, Asashima M, Kurata S, Gehring WJ. Conservation of Pax 6 function and upstream activation by Notch signaling in eye development of frogs and flies. Proc. Natl. Acad. Sci. U. S. A. 2002; 99:2020–2025. [PubMed: 11842182]

Panganiban G, Sebring A, Nagy L, Carroll S. The development of crustacean limbs and the evolution of arthropods. Science. 1995; 270:1363–1366. [PubMed: 7481825]

Philips GT, Stair CN, Young Lee H, Wroblewski E, Berberoglu MA, Brown NL, Mastick GS. Precocious retinal neurons: Pax6 controls timing of differentiation and determination of cell type. Dev. Biol. 2005; 279:308–321. [PubMed: 15733660]

Porter FD, Drago J, Xu Y, Cheema SS, Wassif C, Huang S-P, Lee E, Grinberg A, Massalas JS, Bodine D, et al. *Lhx2*, a LIM homeobox gene, is required for eye, forebrain, and definitive erythrocyte development. Development. 1997; 124:2935–2944. [PubMed: 9247336]

Rachel RA, Dolen G, Hayes NL, Lu A, Erskine L, Nowakowski RS, Mason CA. Spatiotemporal features of early neuronogenesis differ in wild-type and albino mouse retina. J. Neurosci. 2002; 22:4249–4263. [PubMed: 12040030]

Rapaport DH, Wong LL, Wood ED, Yasumura D, LaVail MM. Timing and topography of cell genesis in the rat retina. J. Comp. Neurol. 2004; 474:304–324. [PubMed: 15164429]

Sanes JR, Rubenstein JL, Nicolas JF. Use of a recombinant retrovirus to study post-implantation cell lineage in mouse embryos. EMBO J. 1986; 5:3133–3142. [PubMed: 3102226]

Sasai Y, Kageyama R, Tagawa Y, Shigemoto R, Nakanishi S. Two mammalian helix-loop-helix factors structurally related to *Drosophila hairy* and *Enhancer of split*. Genes Dev. 1992; 6:2620–2634. [PubMed: 1340473]

Schneider ML, Turner DL, Vetter ML. Notch signaling can inhibit Xath5 function in the neural plate and developing retina. Mol. Cell. Neurosci. 2001; 18:458–472. [PubMed: 11922138]

Steingrimsson E, Moore KJ, Lamoreux ML, Ferre-D'Amare AR, Burley SK, Zimring DC, Skow LC, Hodgkinson CA, Arnheiter H, Copeland NG, et al. Molecular basis of mouse microphthalmia (mi) mutations helps explain their developmental and phenotypic consequences. Nat. Genet. 1994; 8:256–263. [PubMed: 7874168]

Tachibana M, Perez-Jurado LA, Nakayama A, Hodgkinson CA, Li X, Schneider M, Miki T, Fex J, Francke U, Arnheiter H. Cloning of MITF, the human homolog of the mouse microphthalmia gene and assignment to chromosome 3p14.1-p12.3. Hum. Mol. Genet. 1994; 3:553–557. [PubMed: 8069297]

Takatsuka K, Hatakeyama J, Bessho Y, Kageyama R. Roles of the bHLH gene Hes1 in retinal morphogenesis. Brain Res. 2004; 1004:148–155. [PubMed: 15033430]

Takebayashi K, Sasai Y, Sakai Y, Watanabe T, Nakanishi S, Kageyama R. Structure, chromosomal locus, and promoter analysis of the gene encoding the mouse helix-loop-helix factor HES-1. J. Biol. Chem. 1994; 269:5150–5156. [PubMed: 7906273]

Tomita K, Ishibashi M, Nakahara K, Ang S-L, Nakanishi S, Guillemot F, Kageyama R. Mammalian hairy and enhancer of split homolog 1 regulates differentiation of retinal neurons and is essential for eye morphogenesis. Neuron. 1996a; 16:723–734. [PubMed: 8607991]

Tomita K, Nakanishi S, Guillemot F, Kageyama R. Mash1 promotes neuronal differentiation in the retina. Genes Cells. 1996b; 1:765–774. [PubMed: 9077445]

Trieu M, Ma A, Eng SR, Fedtsova N, Turner EE. Direct autoregulation and gene dosage compensation by POU-domain transcription factor Brn3a. Development. 2003; 130:111–121. [PubMed: 12441296]

Turner DL, Cepko CL. A common progenitor for neurons and glia persists in rat retina late in development. Nature. 1987; 328:131–136. [PubMed: 3600789]

Turner DL, Snyder EY, Cepko CL. Lineage-independent determination of cell type in the mouse retina. Neuron. 1990; 4:345–833.

Vetter ML, Brown NL. The role of basic helix-loop-helix genes in vertebrate retinogenesis. Cell Dev. Biol. 2001; 12:491–498.

Walther C, Gruss P. Pax-6, a murine paired box gene, is expressed in the developing CNS. Development. 1991; 113:1435–1449. [PubMed: 1687460]

Wang SW, Kim BS, Ding K, Wang H, Sun D, Johnson RL, Klein WH, Gan L. Requirement for math5 in the development of retinal ganglion cells. Genes Dev. 2001; 15:24–29. [PubMed: 11156601]

Watanabe M, Rutishauser U, Silver J. Formation of retinal ganglion cell and optic fiber layers. J. Neurobiol. 1991; 22:85–96. [PubMed: 2010752]

Wetts R, Fraser SE. Multipotent precursors can give rise to all major cell types of the frog retina. Science. 1988; 239:1142–1145. [PubMed: 2449732]

Xiang M, Zhou L, Peng YW, Eddy RL, Shows TB, Nathans J. Brn-3b: a POU domain gene expressed in a subset of retinal ganglion cells. Neuron. 1993; 11:689–701. [PubMed: 7691107]

Yun K, Fischman S, Johnson J, Hrabe de Angelis M, Weinmaster G, Rubenstein JL. Modulation of the notch signaling by Mash1 and Dlx1/2 regulates sequential specification and differentiation of progenitor cell types in the subcortical telencephalon. Development. 2002; 129:5029–5040. [PubMed: 12397111]

Zhang L, Mathers PH, Jamrich M. Function of Rx, but not Pax6, is essential for the formation of retinal progenitor cells in mice. Genesis. 2000; 28:135–142. [PubMed: 11105055]

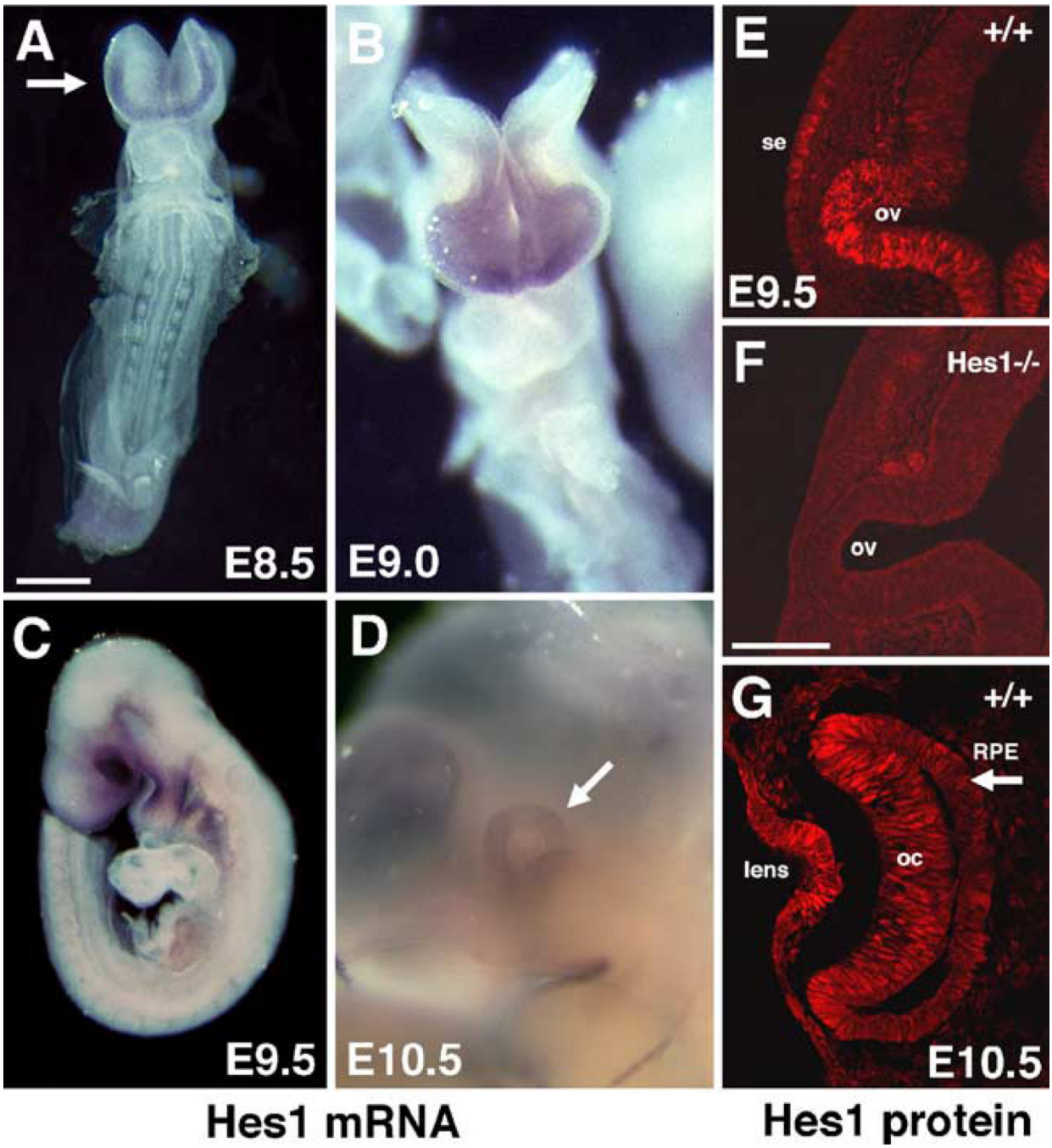

Fig. 1.

Hes1 is expressed at the earliest stages of eye development. (A–D) In situ hybridization for *Hes1* mRNA. Dorsal is up or upper left. (A, B) Frontal views. *Hes1* mRNA is expressed in the E8.5 anterior neural plate (arrow in A) and optic vesicles of E9.0 embryos (B). (C, D) Lateral embryo views with rostral to the left. *Hes1* mRNA is strongly expressed in the E9.5 optic region (C). At E10.5, *Hes1* mRNA persists throughout the optic cup (arrow in D). (E–G) Immunofluorescent antibody labeling with anti-Hes1 antibody. (E, F) Cryosections through E9.5 wild type (E) and *Hes1*−/− (F) optic vesicles. Hes1 protein expression in both

surface ectoderm (se) and optic vesicle (ov) are missing in mutants (F). (G) At E10.5, Hes1 protein expression is apparent in the lens, optic cup (oc), and RPE (arrow). Scale bar = 500 μm in panel A, 20 μm in panel F.

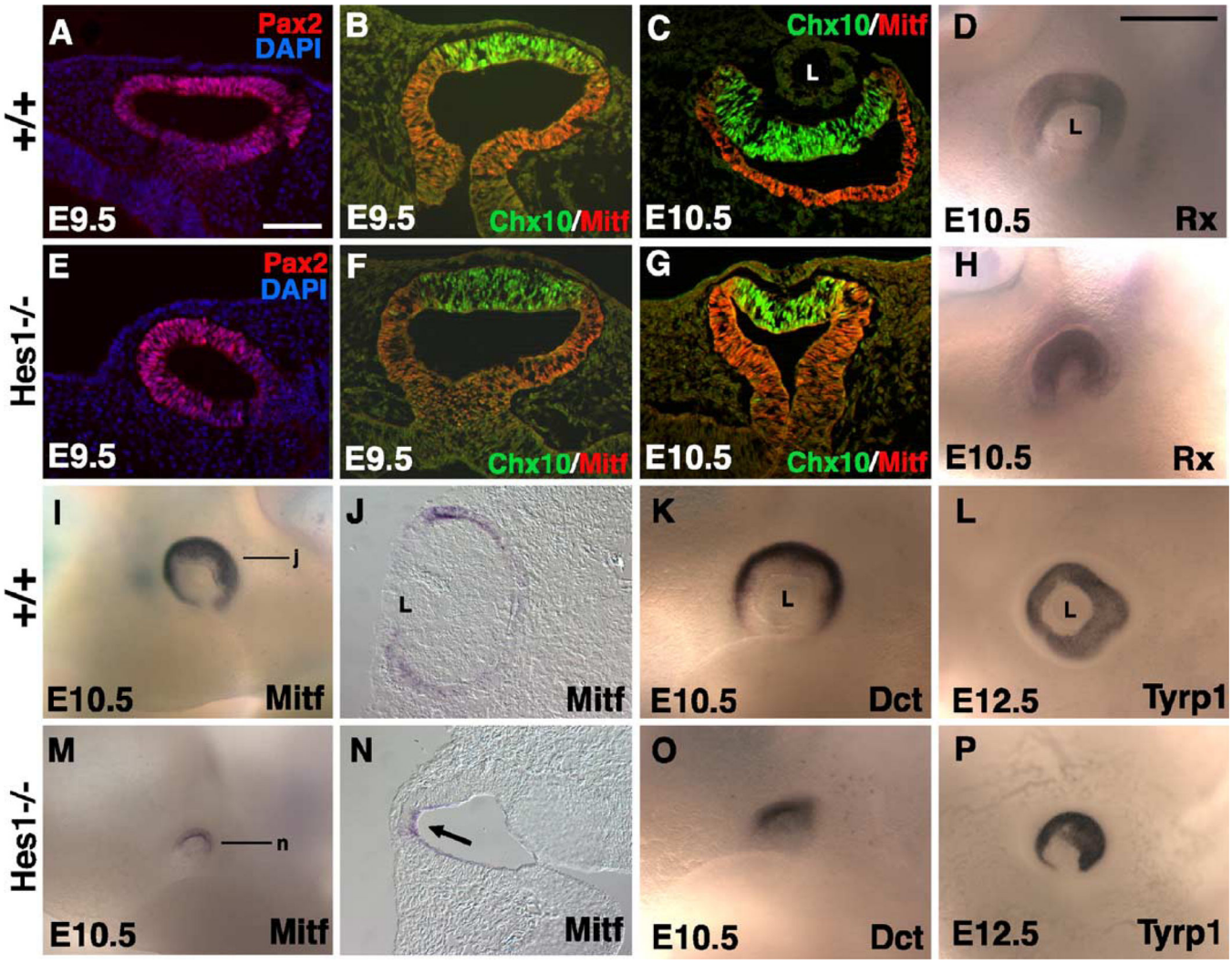

Fig. 2.

Early specification and patterning are normal in *Hes1* mutants. Wild type and *Hes1* mutant embryos labeled with Pax2, Chx10, and Mitf antibodies or in situ hybridization using Rx, Mitf, Dct, and Tyrp1 cRNA probes. In the horizontal sections A–C and E–G, rostral is right and lateral up; in sections D, H–P, rostral is left and dorsal up. (A, E) Pax2 expression (red) in the E9.5 optic vesicle is unaffected in *Hes1* mutant embryos. Sections were also counterstained with DAPI (blue). (B, F) Chx10 (green) and Mitf (red) double labeling at E9.5 demonstrates that retina versus RPE/optic stalk boundaries are unaffected in *Hes1* mutants. (C, G) In E10.5 wild type, morphogenesis of the optic cup and an almost single cell layered RPE are visible (C). In *Hes1* mutants, morphogenesis is arrested at the vesicle stage although retina versus RPE specification is maintained. A few *Hes1* mutants had small numbers of cells co-expressing Chx10 and Mitf (yellow domain in between green and red cells in panel G. (D, H) In E10.5 Hes1−/− eyes, *Rx* mRNA is expressed throughout the future retina as it is in wild type. (I, J, M, N) *Mitf* mRNA expression in the specified RPE is greatly reduced in E10.5 *Hes1*−/− embryos (arrow in N). (K, O) Two markers of differentiating RPE, Dct, and Tyrp1 (not shown) are also reduced in *Hes1* mutants at E10.5.

(L, P) At E12.5, Dct (not shown) and Tyrp1 are clearly expressed but their expression domains smaller than normal in *Hes1* mutants. Scale bar = 20 μm in panels A–C, F, G, J, and N, and 500 μm in panels D, H, I, K–M, O, and P.

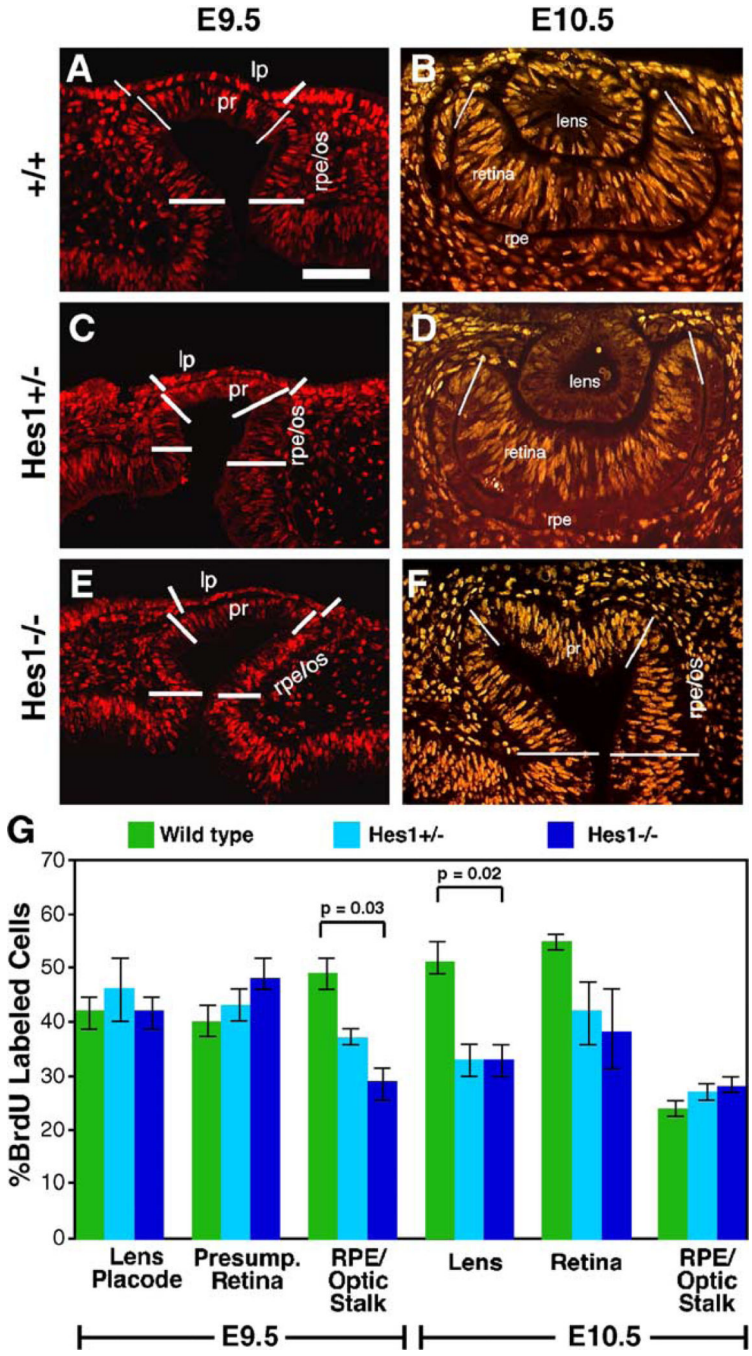

Fig. 3.

Loss of *Hes1* reduces lens and RPE/OS proliferation. Anti-BrdU labeling (in red) of sections containing E9.5 and E10.5 optic regions. White lines in all panels denote tissue boundaries assigned for cell counting. (A, C, E) Representative sections from E9.5 wild type, *Hes1*+/−, and *Hes1*−/− eyes showing BrdU incorporation. (B, D, F) Although the E10.5 *Hes1*−/− eye (F) arrested at the optic vesicle stage, numerous proliferating cells are present. The two shades of red among the sets of images are due to pseudo coloring by different computer imaging programs. (G) The number of cells in S-phase (BrdU antibody labeling) was

divided by the total number of nuclei (DAPI labeling, not shown) to give a labeling index (% BrdU labeled cells) on the *y* axis plotted versus developmental age and tissue type (*x* axis) for wild type, *Hes1*+/−, and *Hes1*−/− embryos. Statistically significant changes for the E9.5 RPE/OS and E10.5 lens are denoted by a bracket and the *P* values obtained using ANOVA and Fisher's test. The black line on each bar of the graph represents standard error of the mean. lp = lens placode, pr = presumptive retina, rpe = retinal pigmented epithelium, rpe/os = region of the optic vesicle that gives rise to both structures. Scale bar = 20 μm in panel A.

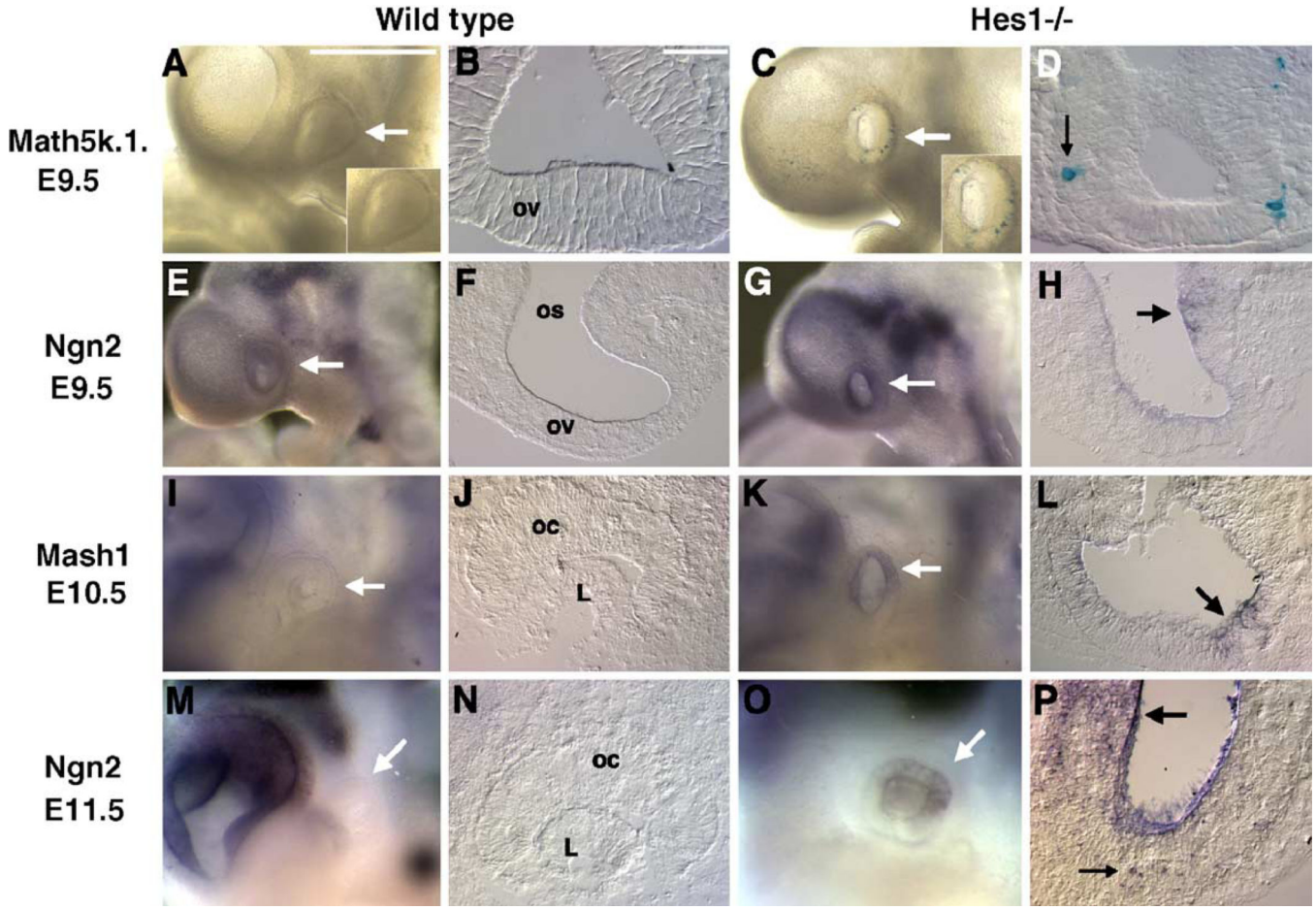

Fig. 4.

Math5, *Ngn2*, and *Mash1* are selectively derepressed in *Hes1* mutants. β-galactosidase or mRNA expression in wild type and *Hes1*−/− optic vesicles (E9.5) and cups (E10.5–11.5), examined in pairs of images of whole mounts and sections. In panels A, C, E, G, I, K, M, and O, nasal is left and dorsal up and white arrows point to the eye. In panels B, D, F, H, J, L, N, and P, medial is up and rostral is left. (A–D) Comparison of 22-somite *Hes1* +/+;*Math5LacZk.i.*/+ and *Hes1*−/−;*Math5lacZk.i.*/+ littermate embryos at E9.5. No β-gal-positive cells are found in control embryos (A, B). Math5lacZ expression is precocious in *Hes1* mutant optic vesicles (C, D). Insets in panels A and C show the optic vesicle at higher magnification. (E–H) *Ngn2* is ectopically expressed in the optic stalk at E9.5. Premature expression of *Ngn2* in cross section through the forming optic stalk of *Hes1* mutants (arrow in H). Precocious *Ngn2* expression is not detected in the optic vesicle/cup at E9.5 or E10.5. (I–L) *Mash1* mRNA is upregulated in a small dorsal domain at E10.5 in *Hes1* mutants. Arrow in panel L denotes a small group of cells inappropriately expressing *Mash1*. (M–P) At E11.5, *Ngn2* mRNA is ectopically expressed in both the optic cup and stalk. *Ngn2* expression is upregulated in a *Hes1* mutant with a nearly normal optic cup (O). Cross section through an E11.5 *Hes1* mutant eye with arrested morphogenesis and ectopic *Ngn2* expression in the optic vesicle (thin arrow) and stalk (thick arrow). Scale bar in panel A = 500 μm, panel B = 50 μm.

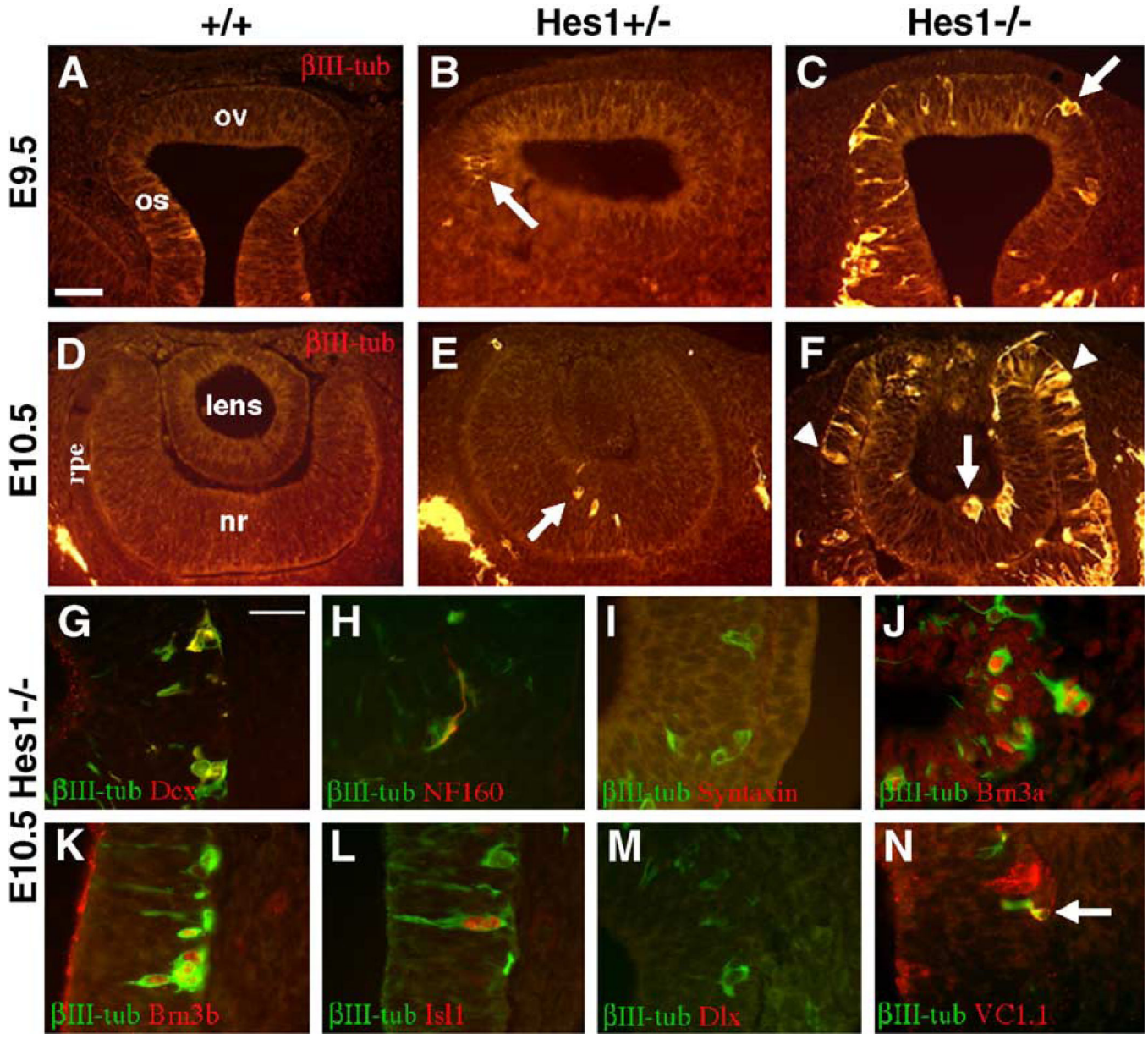

Fig. 5.

Early retinal neuron cell types have accelerated differentiation in *Hes1* mutants. Antibody labeling with anti-βIII-tubulin, an early marker of neuronal differentiation. Wild type optic vesicle (A) and cup (D) sections do not contain neurons at these stages. (A–C) Anti-βIII-tubulin labeling at embryonic day 9.5 (E9.5) demonstrates the presence of a few precocious neurons in Hes1 heterozygotes (arrow in B) but many more in homozygous mutants (C). Differentiating neurons often exhibit neuronal morphology, including neurite extension (arrow in C). (D–F) E10.5 optic cups in wild type, heterozygous, and homozygous *Hes1* mutants. *Hes1*+/− and *Hes1*−/− optic cups have precocious neurons (arrows), with many more in homozygous mutants. Ectopic neurons in *Hes1* mutant are also found in the optic stalk (C) and RPE (arrowheads in F). (G–N) Optic cup sections of E10.5 *Hes1*−/− embryos, with vitreal to the right. (G) βIII-tubulin (green) and the RGC marker Doublecortin (red)

completely overlap (yellow). (H) Co-labeling with the RGC marker NF-160 and βIII-tubulin further indicates that precocious neurons exhibit RGC characteristics. (I) βIII-tubulin+ cells do not express the amacrine cell marker Syntaxin. (J, K) Double-labeling with βIII tubulin and RGC markers Brn3a (J) or Brn3b (K) indicate that the neurons express both markers. (L) βIII-tubulin+ neurons also express Isl1, found in RGCs, and amacrine neurons. (M) Dlx, a marker for early RGCs, horizontal, amacrine, and bipolar neurons in wild type is not expressed in *Hes1*−/− optic vesicles. (N) *Hes1*−/− cells expressing either the amacrine/horizontal cell marker VC1.1 alone (red cells) or both βIII-tubulin and VC1.1 (arrow points to the co-labeling in yellow). rpe = retinal pigmented epithelium, nr = neural retina, ov = optic cup, os = optic stalk. Scale bar = 50 μm in panel A, 20 μm in panel G.

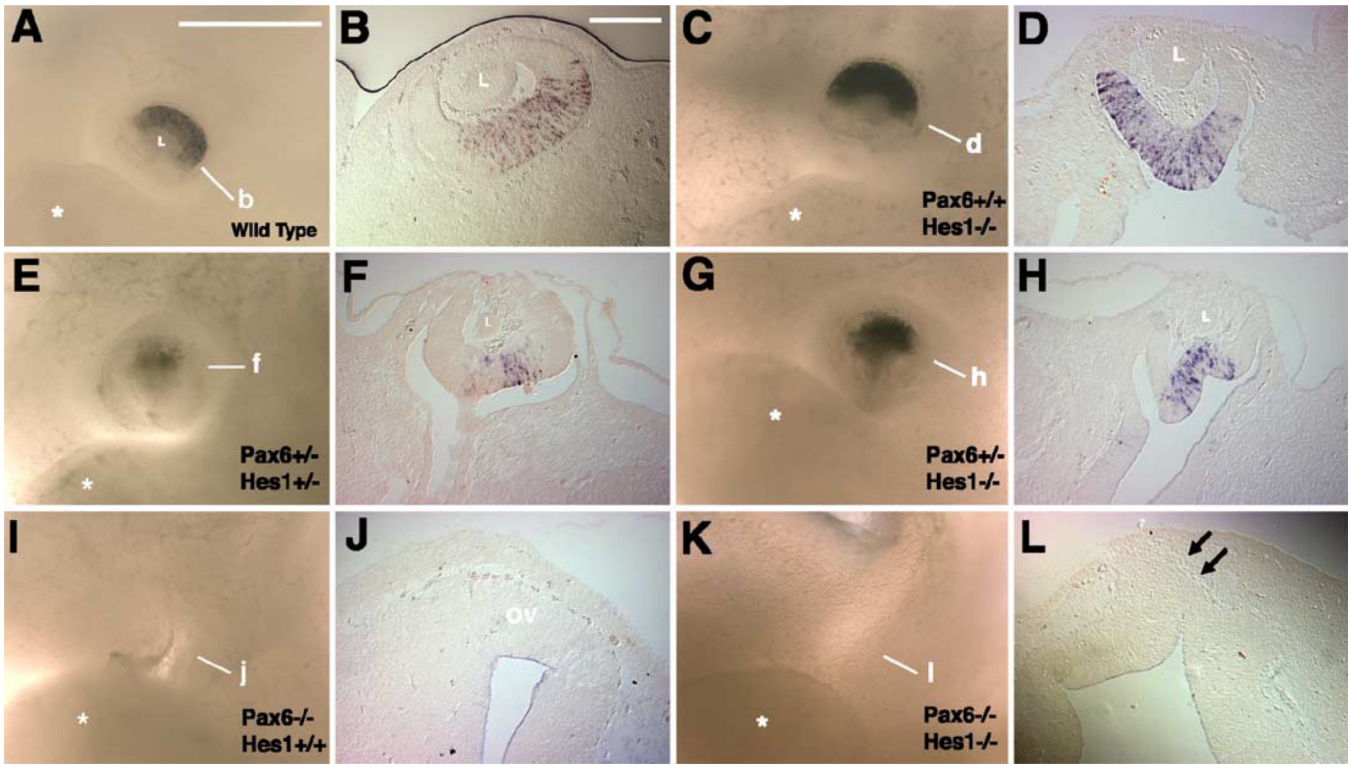

Fig. 6.

Hes1 and *Pax6* regulation of *Math5*. *Math5* in situ hybridization of E11.0 embryos with differing dosages of *Pax6* and *Hes1*. Panels A, C, E, G, I, and K are whole-mount images of the optic region with nasal left and dorsal up. A white line depicts the plane of section shown in panels B, D, F, H, J, and L horizontal sections from the embryo in each preceding panel, with lateral up. (A, B) Wild type *Math5* expression in the dorsal optic cup. (C, D) A *Hes1* homozygous mutant with strong *Math5* expression. (E, F) In embryos with one mutant copy of *Pax6* and *Hes1*, eyes are smaller than wild type with few *Math5*-expressing cells. This phenotype is identical to *Pax6* heterozygotes (Brown et al., 1998). (G, H) An abnormal optic cup in *Pax6*+/−;*Hes1*−/− embryos, where *Math5*-expressing cells are numerous compared to double heterozygotes. The only difference between eyes in panels E and F, and G and H is increasing loss of *Hes1*. (I, J) In single *Pax6* mutants, all *Math5* expression is absent. Note arrested optic vesicle development compared to panels A–H. (K, L) Embryos mutant for both *Pax6* and *Hes1* completely lack an eye. In serial sections, only a slight evagination of the diencephalon could be found (arrows). L = lens, ov = optic vesicle, asterisks indicate forming brachial arch in panels A, C, E, G, I, and K. Scale bar = 500 μm in panel A, 50 μm in panel B.

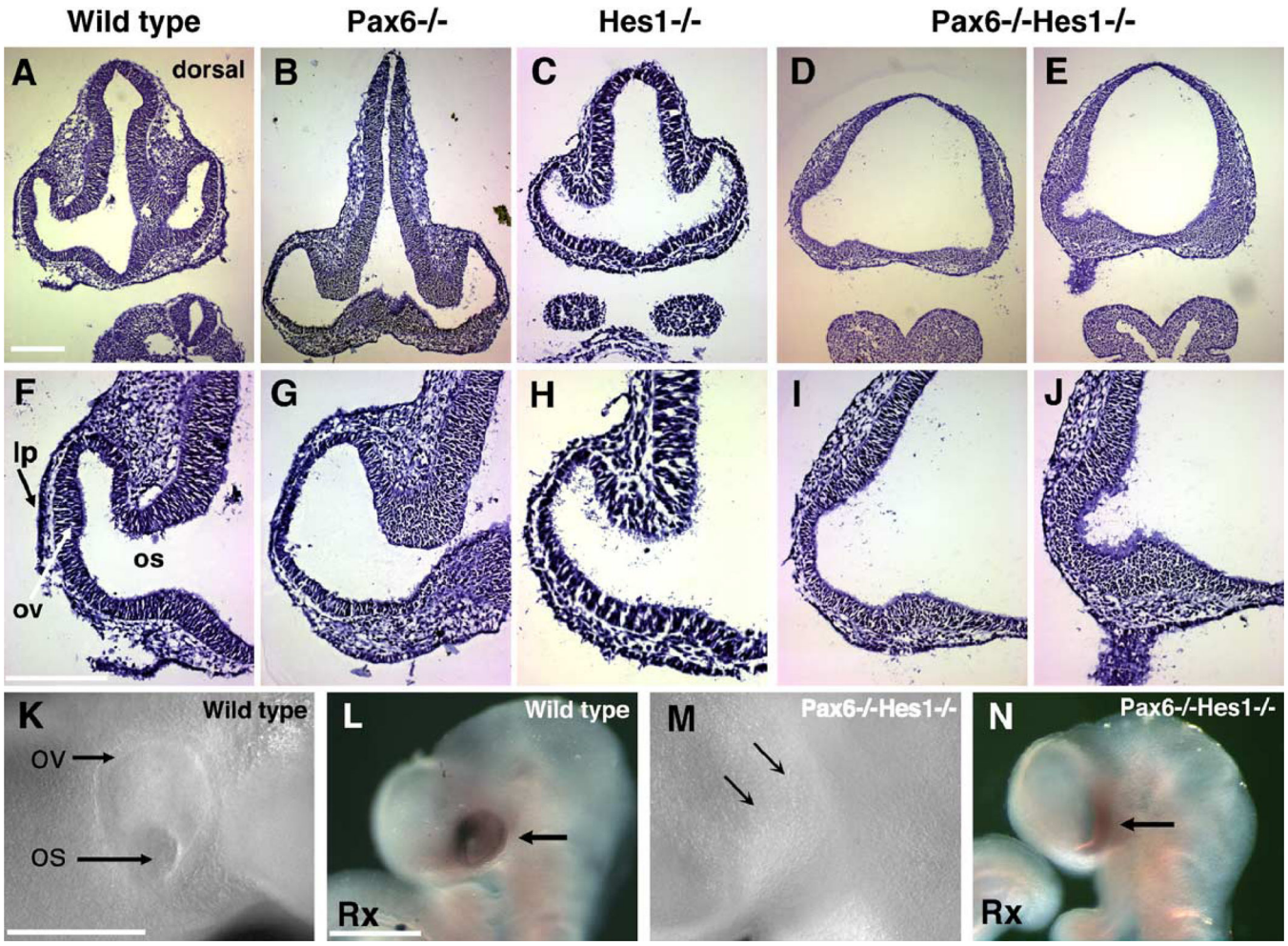

Fig. 7.

Hes1/Pax6 double mutant embryos lack optic vesicles. (A–J) Hematoxylin-stained 10-μm frontal sections through the optic region of E9.5 embryos. Panels F–J are higher magnifications of the same sections. (A, F) 28-somite wild type embryo sections containing lens placode (lp), optic vesicle (ov), and optic stalk (os). (B, G) 27-somite *Pax6*−/− embryo that lacks a lens placode and has open optic vesicle morphology (G). (C, H) *Hes1*−/− 22-somite embryo with a missing lens placode and abnormal optic vesicle shape (H). (D, E, I, J) A *Pax6*−/−*Hes1*−/− 24-somite embryo at two different section depths (panels D, I are more rostral than panels E, J). A narrow bulge of the diencephalon neural tube is seen in 1 –2 sections per embryo (J). Otherwise, these embryos lack a recognizable optic vesicle and exhibit abnormal fore- and hindbrain formation (not shown). (K–N) Whole-mount images of live embryos (K, M) or embryos post-*Rx* in situ hybridization (L, N). Image in panel K is of the embryo sectioned in panels A and F, the image in panel M is of the embryo in panels D, E, I, and J. At the surface ectoderm of the double mutant embryo, arrows point to the position where the optic vesicle and lens placode should be observable. In panel N, a band of cells express *Rx* (arrow), thus are specified for optic fate. Scale bar = 50 μm in panels A and G, 500 μm in panels K and L.

Table 1

Molecular epistasis of Hes1, Pax6, Rx, and Math5 from E8.5 to E12.5

mRNA expression	Mutation			
	Rx	**Pax6**	**Hes1**	**Math5**
Rx	NA	Normal[a]	Normal	Normal
Pax6	Downregulated[a]	NA	Normal	Normal
Hes1	Not tested	Normal E8.5–E10 Upregulated E10.5–E11.5[b]	NA	Normal
Math5	Not tested	Downregulated at E11[b]	Upregulated at E9.5	NA

NA = not applicable.

[a] Zhang et al. (2000).

[b] Brown et al. (1998).